



# Cobalt containing crystallizing glass seals for solid oxide fuel cells – A new strategy for strong adherence to metals and high thermal expansion



Christian Thieme, Christian Rüssel\*

Otto-Schott-Institut, Jena University, Fraunhoferstr. 6, 07743 Jena, Germany

## HIGHLIGHTS

- Cobalt and barium containing silicate glasses were prepared.
- The powdered glasses could be fully densified during sintering.
- At the end of sintering barium and cobalt containing crystals were precipitated.
- At the interface, cobalt ions were reduced by the microfer alloy to metallic cobalt.
- The glasses exhibit high thermal expansion and strong adherence to the metal.

## ARTICLE INFO

### Article history:

Received 11 October 2013

Received in revised form

13 January 2014

Accepted 6 February 2014

Available online 18 February 2014

### Keywords:

Solid oxide fuel cells

Crystallizing glass seals

Thermal expansion

Barium silicates

Barium cobalt zinc silicates

## ABSTRACT

Powdered glasses based on the systems BaO/CoO/SiO<sub>2</sub> and BaO/ZnO/CoO/SiO<sub>2</sub> with small additions of ZrO<sub>2</sub>, La<sub>2</sub>O<sub>3</sub> and B<sub>2</sub>O<sub>3</sub> were investigated with respect to their sintering and crystallization behavior. They could be fully densified by viscous flow and during subsequent crystallization BaSi<sub>2</sub>O<sub>5</sub> and Ba(Zn<sub>x</sub>Co<sub>2-x</sub>)Si<sub>2</sub>O<sub>7</sub> or BaCo<sub>2</sub>Si<sub>2</sub>O<sub>7</sub> were formed. The CTEs (100–800 °C) of crystallized samples were 14.0–14.6 × 10<sup>-6</sup> K<sup>-1</sup>. Sealing experiments with Nicrofer<sup>®</sup> alloy showed strong adherence of the crystallized glass. Aluminum from the alloy is oxidized and forms an alumina layer or interconnected structures inside the metal. Cobalt oxide as a component of the glass is reduced to the metal and occurs as approximately spherical particles near the Nicrofer<sup>®</sup> alloy. The number of cobalt particles increases with increasing sealing temperature. During fracture of sealed Nicrofer<sup>®</sup> plates, the crack runs through the glass and not through the interface metal/crystallized glass.

© 2014 Elsevier B.V. All rights reserved.

## 1. Introduction

Joining of materials, such as metals or ceramics [1] is frequently done by glasses. This is of great importance especially for solid oxide fuel cells (SOFCs) and other chemical reactors which are used at high temperatures typical in the range from 700 to 1000 °C [2]. For this purpose, the glass is powdered and brought in between the materials to be joined. Then this arrangement is thermally annealed which leads to a densification (sintering) by viscous flow.

Unfortunately, there seems to be a certain correlation between the coefficient of thermal expansion (CTE) and the glass transition temperature,  $T_g$  (or the softening temperature) [1]. Usually, glasses

with high  $T_g$  (>750 °C) possess fairly low CTE [3,4], while glasses with high CTE (>12 × 10<sup>-6</sup> K<sup>-1</sup>) exhibit low  $T_g$  and hence fairly small softening temperatures [5–9].

In the case of solid oxide fuel cells or other high temperature reactors, metals are to be joint, which commonly have CTEs >11 × 10<sup>-6</sup> K<sup>-1</sup> [10,11] and the operating temperatures are in the range from 700 to 1000 °C [12]. Glasses, however, which fulfill these two requirements, are not available and seals which during applications contain only amorphous phases cannot be applied.

Seals which might fulfill these two requirements do not only contain a glassy phase, but additionally at least one crystalline phase. Such materials, in principle, might be prepared using two different ways: a crystalline phase of high thermal expansion coefficient is given to the glass and then thermal treatment is carried out which leads to densification by viscous flow [13]. This procedure works well if the volume percentage of crystalline phase is not

\* Corresponding author. Tel.: +49 03641 9 48500; fax: +49 03641 9 48502.  
E-mail address: [ccr@rz.uni-jena.de](mailto:ccr@rz.uni-jena.de) (C. Rüssel).

too high (<30%) because otherwise densification is difficult to achieve [14]. The second possible way is to precipitate a crystalline phase from the glass after the densification by sintering is completed [15]. The starting material in this case is a homogeneous glass. Materials prepared according these two different ways are usually denominated as “composite seals” or “crystallizing seals”, respectively [2,16].

For crystallizing seals, a glass is melted, crushed and powdered. Then it is brought between the materials to be joined. During subsequent thermal treatment, crystallization should not occur in a notable extend until complete densification is achieved [17]. Subsequently, the seal is crystallized. In order to accelerate crystallization, the latter step might also be carried out at another temperature than the densification step.

In summary, the glass composition and the temperature/time schedule have to be optimized in order to control densification and crystallization. Furthermore, the grain size and grain size distribution have to be adjusted to the respective glass composition, procedure and application.

Crystallizing glasses for solid-oxide fuel cells must be stable at high temperatures (typically  $\geq 850^\circ\text{C}$ ) over a long period of time (many years). The softening temperature of the seal should be above the operating temperature [18,19]. The CTEs of the crystallized seal and of the different components of the cell should be in agreement within  $\pm 1 \cdot 10^{-6} \text{ K}^{-1}$  [18].

In SOFCs as cathode mostly perovskites such as  $\text{La}_{1-x}\text{Sr}_x\text{CoO}_{3\pm\delta}$  are used [20]. Their CTEs (30–800  $^\circ\text{C}$ ) are typical in the range from  $11$  to  $14 \times 10^{-6} \text{ K}^{-1}$  [19,21]. As anode, a cermet of nickel and stabilized zirconia is used. The CTE (25–1000  $^\circ\text{C}$ ) is in the range from  $12.7$  to  $13.3 \times 10^{-6} \text{ K}^{-1}$  for a nickel concentration of 30–45 wt% [22]. The interconnect in SOFCs is commonly composed by different heat- and oxidation resistant materials such as Ni-based alloys [23], exhibiting CTEs in the range from  $14$  to  $19 \times 10^{-6} \text{ K}^{-1}$  [10].

Besides a good matching of CTEs, strong adherence between the seal and the different cell components is required for the long-term stability of an SOFC. This paper reports on glasses with high CoO concentrations. CoO is commonly known as an adherence promoting oxide for improving the adhesion between metals (mostly steels) and vitreous enamels [24]. In the following, an attempt is introduced in which the effect of CoO in enamels is transferred to a crystallizing sealing glass of an SOFC. The CoO as a component of the glass composition is in a later stage incorporated into a crystal phase.

This paper reports on glasses based on the system  $\text{BaO}/\text{ZnO}/\text{CoO}/\text{SiO}_2$ . The densification, the crystallization behavior, the microstructure and the thermal expansion of the crystallized samples are described. Furthermore, the glass is used for joining a high temperature alloy suitable as interconnect for SOFCs.

## 2. Materials and methods

The glasses were prepared from reagent grade raw materials. Mixtures of  $\text{SiO}_2$ ,  $\text{BaCO}_3$  (VK Labor- und Feinchemikalien),  $\text{ZnO}$  (Carl Roth GmbH + Co. KG, Karlsruhe),  $\text{Co}_3\text{O}_4$  (pure, VEB Laborchemie Apolda),  $\text{ZrO}_2$  (E. Merck, Darmstadt),  $\text{La}_2\text{O}_3 \cdot \text{H}_2\text{O}$  (VEB Laborchemie

Apolda) and  $\text{H}_3\text{BO}_3$  (E. Merck, Darmstadt) were used. They were melted in batches of 50 g in a platinum crucible at a temperature of  $1580^\circ\text{C}$ , kept for 1 h. Then the glasses were cast on a copper block and transferred to a furnace preheated to  $700^\circ\text{C}$ , which was subsequently switched off in order to allow the sample to cool. The batch compositions and the compositions determined by EDX-analysis (standardless measurement) of the studied glasses are given in Table 1.

The glasses were annealed at temperatures of 920 or  $950^\circ\text{C}$ , kept for 1 h. The powdered (grain size  $< 63 \mu\text{m}$ ) and annealed samples were studied by X-ray powder diffraction (XRD), using a SIEMENS D5000 diffractometer with  $\text{Cu K}_\alpha$  radiation. The patterns were recorded in the  $2\theta$ -range from  $10$  to  $60^\circ$  with a step width of  $0.02^\circ$ . The XRD-patterns were analyzed using the software DIF-FRAC.EVA from BRUKER.

The dilatometric measurements (heating rate  $5 \text{ K min}^{-1}$ ) were performed using a dilatometer NETZSCH Dil 402 PC. For the determination of the glass densities a MICROMERITICS AccuPyc 1330 pycnometer was used. The thermal properties were measured with a home-made DTA apparatus. For the determination of the sintering behavior a side-view hot-stage microscope was used. Using this device, images of the projection of a cylindrical shaped powder compact are made during heating the sample from room-temperature to a temperature above that attributed to the maximum densification.

To study the performance as a sealing material, the glass was powdered and sieved to grain sizes  $< 71 \mu\text{m}$ . Then it was given to a cavity drilled in a plate ( $15 \times 15 \times 2.5 \text{ mm}^3$ ) of a heat resistant alloy and slightly densified using a spatula. The alloy selected for the joining experiments was Nicrofer<sup>®</sup> 6025 HT – alloy 602 CA from ThyssenKrupp VDM. The metal with the powdered glass was heated up to temperatures between  $865$  and  $945^\circ\text{C}$  using a heating rate of  $5 \text{ K min}^{-1}$ . The temperature was kept for 40 min. The sealing procedure was carried out in a silica tube with an inner diameter of  $5.5 \text{ cm}$  flushed with argon. The as prepared samples were cut and the cut planes were subsequently ground and polished.

The microstructures of the sealed samples especially near the interface metal/crystallized glass were studied using scanning electron microscopy (SEM Jeol JSM 7001F).

For the determination of the long-term behavior all the samples described above were prepared twice and were heated using a heating rate of  $5 \text{ K min}^{-1}$  up to  $(840 \pm 10)^\circ\text{C}$ , kept for 300 h in air. The chosen temperature is a typical SOFC operating condition. The samples annealed for 300 h are called A300 and B300.

In order to measure the strength of the composite, samples schematically shown in Fig. 1, were prepared. The sealing temperature was  $865^\circ\text{C}$  kept for 40 min. The mechanical testing carried out is schematically displayed in Fig. 1(6). For this purpose, a mechanical testing machine ZWICK 1445 was used.

## 3. Results and discussion

The glasses had black color and according to the recorded XRD patterns were amorphous. From thin sections of the glass UV–vis–NIR spectra were recorded and showed solely lines attributed to

**Table 1**  
Glass compositions in Mol-%.

Sample	ZnO	CoO	BaO	SiO <sub>2</sub>	B <sub>2</sub> O <sub>3</sub>	ZrO <sub>2</sub>	La <sub>2</sub> O <sub>3</sub>
A (batch)	8.5	8.5	26	54	1	1	1
A (EDX)	$9.1 \pm 1.7$	$9.8 \pm 1.0$	$24.3 \pm 1.1$	$55.4 \pm 1.8$	— <sup>a</sup>	$0.5 \pm 0.2$	$1.1 \pm 0.3$
B (batch)	—	17	26	54	1	1	1
B (EDX)	—	$17.15 \pm 1.3$	$23.03 \pm 1.2$	$58.4 \pm 2.5$	— <sup>a</sup>	$0.6 \pm 0.2$	$0.8 \pm 0.2$

<sup>a</sup> B<sub>2</sub>O<sub>3</sub> could be detected but was not quantified.

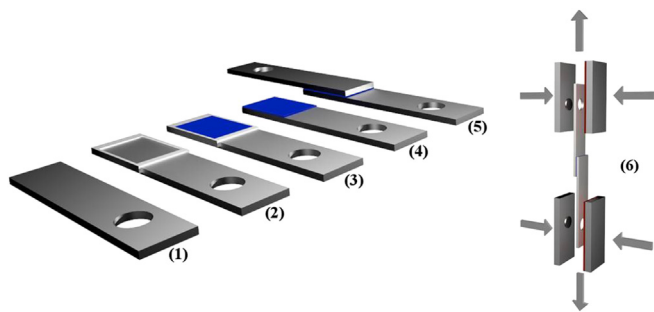


**Fig. 1.** Preparation of samples and mechanical testing: (1) Metal plate consisting of Nicrofer<sup>®</sup> with a size of (16 × 75) mm<sup>2</sup>. (2) Metal plate with a mask consisting of aluminum on it. (3) Mask filled with glass powder (<71 μm). (4) Removal of the mask. The glass layer has a height of 1 mm and a length of 20 mm. (5) Overlapping metal plate on the glass layer. (6) Mechanical testing of the composites. The cylinders on the left jaws serve as a fixation of the samples. The red coating on the right jaws consists of rubber which protects the samples against excessive distortion during clamping and mechanical testing. (For interpretation of the references to color in this figure legend, the reader is referred to the web version of this article).

Co<sup>2+</sup>, a broad absorption line attributed to Co<sup>3+</sup> centered at around 380 nm was not observed. Hence, despite of the used raw material, cobalt occurred entirely as Co<sup>2+</sup>. The densities of the glasses A (zinc and cobalt) and B (only cobalt) were 4.01 and 3.98 g cm<sup>-3</sup>, respectively. The glass transition temperature,  $T_g$ , determined by dilatometry, was 679 °C for glass A and 660 °C for glass B. The dilatometric softening temperatures were 725 and 695 °C for glasses A and B, respectively. The measured DTA profiles showed an exothermic peak with an onset at 901 (glass A) and 862 °C (glass B).

Fig. 2 shows XRD-patterns of samples A and B annealed at 950 and 920 °C, respectively, as well as the samples A300 and B300 where an additional heating step at 840 °C was performed. It should be noted that according to the DTA-profile, the exothermic

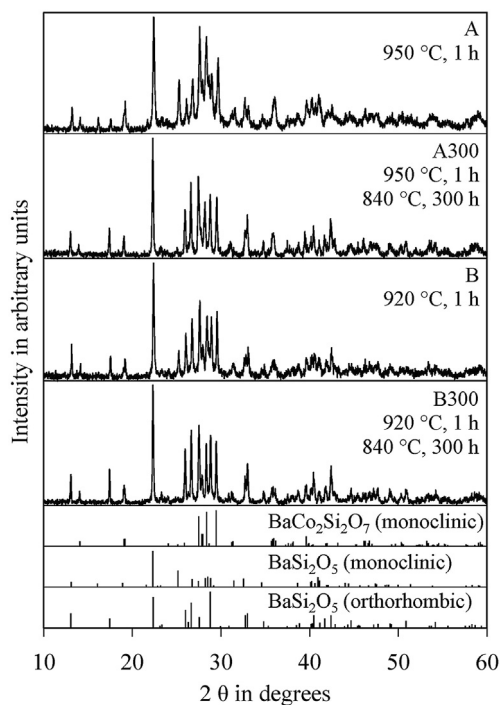


**Fig. 2.** XRD-patterns of samples A, A300, B and B300 after the respective heat treatment. The three patterns in the lower part of the diagram show the most intense theoretical peaks of the respective crystal phases.

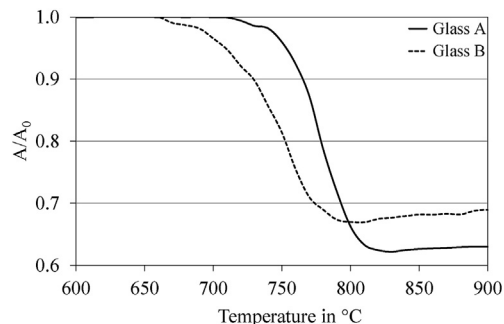


**Fig. 3.** Hot-stage microscopy of the glasses A and B.

peak occurs in sample B at a lower temperature than in sample A. Therefore, for better comparison, sample B and B300 were annealed at a 30 K lower temperature (920 °C).

In the XRD-patterns of the samples A and B numerous distinct lines are observed which show a high degree of crystallinity.

In sample A, the crystalline phases BaCo<sub>2</sub>Si<sub>2</sub>O<sub>7</sub> (monoclinic, JCPDS no. 01-082-0184), BaSi<sub>2</sub>O<sub>5</sub> (monoclinic, JCPDS no. 01-083-1446) as well as BaSi<sub>2</sub>O<sub>5</sub> (orthorhombic, JCPDS no. 00-026-0176) were detected. The monoclinic BaSi<sub>2</sub>O<sub>5</sub> is a high temperature phase, and according to the phase diagram is stable at temperatures above 1350 °C [25].

It should be noted that BaCo<sub>2</sub>Si<sub>2</sub>O<sub>7</sub> and BaZn<sub>2</sub>Si<sub>2</sub>O<sub>7</sub> form solid solutions Ba(Zn<sub>x</sub>Co<sub>2-x</sub>)Si<sub>2</sub>O<sub>7</sub> in the whole concentration range (0 ≤ x ≤ 2) [26]. Since the ionic radii of Co<sup>2+</sup> and Zn<sup>2+</sup> are nearly identical, also the lattice constants of the solid solutions do not depend much on the composition and hence it is scarcely possible to conclude from the XRD-patterns on the composition of the solid solution. Since sample B does not contain zinc, the attribution is clear, however, concerning sample A, it is highly probable that sample A contains a solid solution Ba(Zn<sub>x</sub>Co<sub>2-x</sub>)Si<sub>2</sub>O<sub>7</sub>.

The XRD-patterns of the samples A300 and B300 do not show the peaks of the monoclinic high temperature modification of BaSi<sub>2</sub>O<sub>5</sub>. This is most clearly indicated by the disappearance of the peaks at  $2\theta = 16.1^\circ$ ,  $21.6^\circ$ ,  $25.2^\circ$  and  $32.6^\circ$ . Hence, the long heat treatment at 840 °C leads to the transformation of high temperature BaSi<sub>2</sub>O<sub>5</sub> to low temperature BaSi<sub>2</sub>O<sub>5</sub>.

Fig. 3 shows the results from the hot stage microscopy recorded during densification of uniaxial pressed powders of the samples A and B.  $A_0$  and  $A$  are the areas of the projection of the cylindrical powder compacts before the beginning of the sintering and during annealing, respectively. Densification starts at a temperature of 710 °C for sample A and 660 °C for sample B. At temperatures of 830

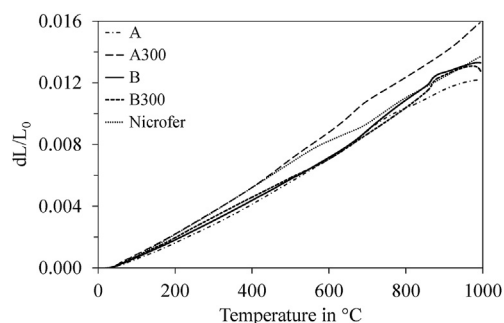


**Fig. 4.** Thermal expansion of samples A and B, crystallized at 950 and 920 °C, kept for 1 h. The samples A300 and B300 were prepared in the same way as the samples A and B, but they were subsequently heated up to 840 °C, kept for 300 h. The thermal expansion of the Nicrofer<sup>®</sup> alloy is also shown.

**Table 2**  
CTEs of the studied crystallized glasses and Nicrofer®.

Temperature range in °C	CTE in $10^{-6} \text{ K}^{-1}$				
	Nicrofer®	Sample A	Sample A300	Sample B	Sample B300
100–300	14.5	11.1	14.0	11.9	12.7
100–600	14.9	12.9	15.9	12.9	12.6
100–800	14.6	14.0	16.4	14.6	13.8
100–900	14.6	13.8	16.4	15.0	14.7
100–1000	14.5	13.0	16.7	14.1	13.2

and 800 °C, the densification is completed and the samples exhibit residual porosities of less than 5%, investigated by SEM micrographs.

Fig. 4 shows dilatometric curves of samples crystallized at 950 °C (A and A300) and at 920 °C (B and B300) before and after a heat treatment of  $(840 \pm 10)^\circ\text{C}$ , kept for 300 h. For comparison also the dilatometric curve of Nicrofer® is shown. In Table 2, the CTEs for different temperature intervals are shown for samples A, B, A300, B300 and the alloy. Within the temperature range from 100 to 800 °C the CTEs of the crystallized glasses A, B and the alloy are all in the range from  $14.0$  to  $14.6 \times 10^{-6} \text{ K}^{-1}$ . The crystallizing seals fit well to the Nicrofer® alloy with respect to the thermal expansion.

After 300 h of heat treatment the dilatometric behavior of sample A has changed significantly (see sample A300 in Fig. 4). Generally the trend is the same, but the dilatation is somewhat higher, resulting in CTEs being  $(2.4\text{--}3.7) \cdot 10^{-6} \text{ K}^{-1}$  higher than before the heat treatment. Most probably this is due to a more complete crystallization as well as to the above mentioned phase transition of high temperature  $\text{BaSi}_2\text{O}_5$  to low temperature  $\text{BaSi}_2\text{O}_5$  after 300 h. Between room temperature and 500 °C the thermal expansion behavior of sample A300 fits very well with the behavior of Nicrofer®. The thermal treatment at 840 °C has only a minor effect on the dilatation of the sample B. The maximum difference of the CTEs of samples B and B300 is  $0.9 \cdot 10^{-6} \text{ K}^{-1}$ . This small difference in the CTE-values might be caused by different crystal orientations in the samples as well as the as mentioned phase transition

[26]. Furthermore, the steep increase in length of the samples B and B300 at around 850 °C corresponds to a phase transition known from  $\text{BaCo}_2\text{Si}_2\text{O}_7$  [26]. This phase transition results in relatively small changes in the sample volume in comparison with similar crystal phases such as  $\text{BaZn}_2\text{Si}_2\text{O}_7$  [19]. However, this phase transition might induce stresses into the sealing material.

For sealing experiments, temperatures in the range from 865 to 945 °C were chosen. The samples were subsequently cut, ground and polished and especially near the interface with the metal characterized using SEM. In Fig. 5, micrographs of samples prepared from the glasses A and B and the Nicrofer® alloy at temperatures of 865, 920 and 945 °C are shown. The upper part of each micrograph shows the metal, while the lower part shows the crystals precipitated from the glass and supposedly some residual glassy phase. In the lower part of all samples, near the metal numerous small spots of bright appearance are observed. The number of observed spots is higher in samples prepared from glass B than in those prepared from glass A. Increasing sealing temperatures also led to an increasing number of spots. The formation of the bright spots runs parallel to the formation of interconnected structures of dark appearance in the metal.

Fig. 6 shows EDX patterns of a sample prepared from Nicrofer® and glass A at 945 °C. The respective patterns are attributed to Al, Ba, Co, Cr, Fe, La, Ni, O, Si, Zr and Zn (the concentrations, see scale on the right, are given in wt%). The measured concentrations have a relative error of around 5%. The minimum uncertainties are around 0.1 wt%. The boundary between the metal and the crystallized glass appears dark and is strongly enriched in aluminum. Besides, notable quantities of oxygen occur in this phase. Hence it is mainly alumina. The bright spots already observed in the micrographs shown in Fig. 5 are mainly composed of metallic cobalt; all other elements, including oxygen do not occur in notable concentrations in these spots. Furthermore, in the SEM, the particles appear even a little bit brighter than the Nicrofer® alloy and are hence definitely not an oxidic compound. Concerning the crystallized glassy phase, notable differences in the chemical composition occur: one phase is enriched in cobalt and zinc. Besides, notable quantities of silicon and barium as well as oxygen occur. The simultaneous occurrence

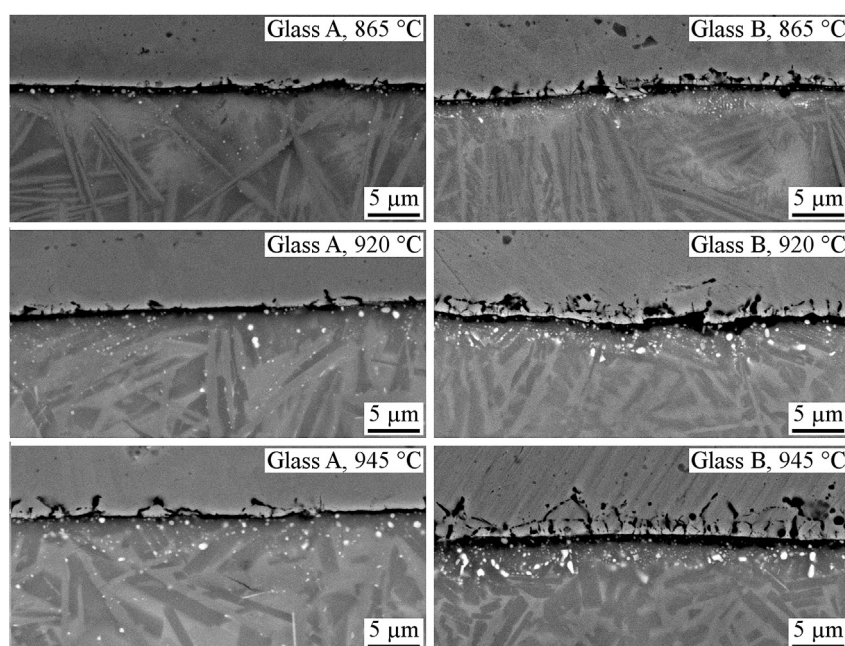


**Fig. 5.** SEM-micrographs of samples A (left) and B (right) sealed at 865, 920 and 945 °C (bottom: crystallized glass, top: metal).

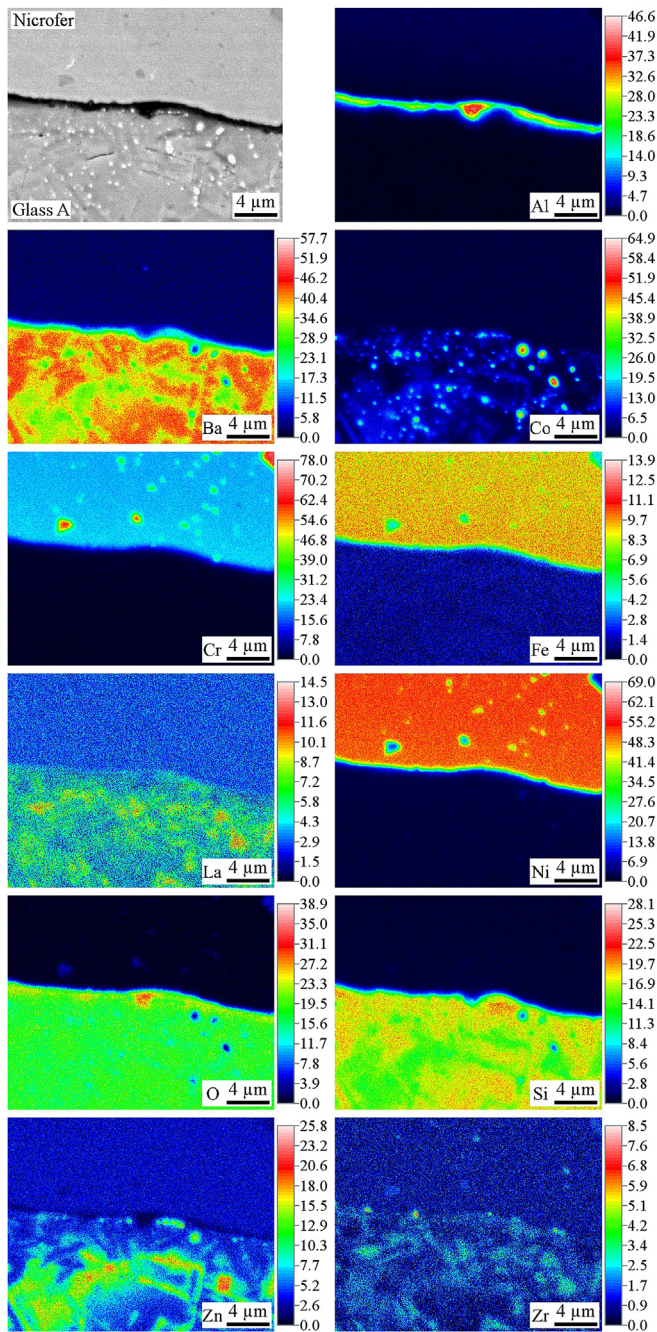


**Fig. 6.** SEM-micrograph and EDX mappings of sample A, sealed to the metal at 945 °C Al, Ba, Co, Cr, Fe, La, Ni, O, Si, Zr and Zn (the concentrations are given in wt%).

of Zn and Co in this sample is a strong hint of the formation of a solid solution [27]. This phase is most probably the solid solution  $\text{Ba}(\text{Zn}_x\text{Co}_{2-x})\text{Si}_2\text{O}_7$  which gave rise to XRD-patterns similar to  $\text{BaCo}_2\text{Si}_2\text{O}_7$ . Another crystalline phase contains mainly barium, silicon and oxygen. This should be the  $\text{BaSi}_2\text{O}_5$  phase observed in the XRD-patterns. Lanthanum and zirconium are depleted in those regions, the barium concentrations are highest.

In Fig. 7, EDX-patterns of the sample prepared from Nicrofer® and glass B are shown. The detected elements are the same as in Fig. 6, (besides Zn, which does not occur in this sample). The bright spots are more numerous than in Fig. 6 and by analogy are composed of metallic cobalt. Within the limits of the method applied other elements are not detected within these bright spots.

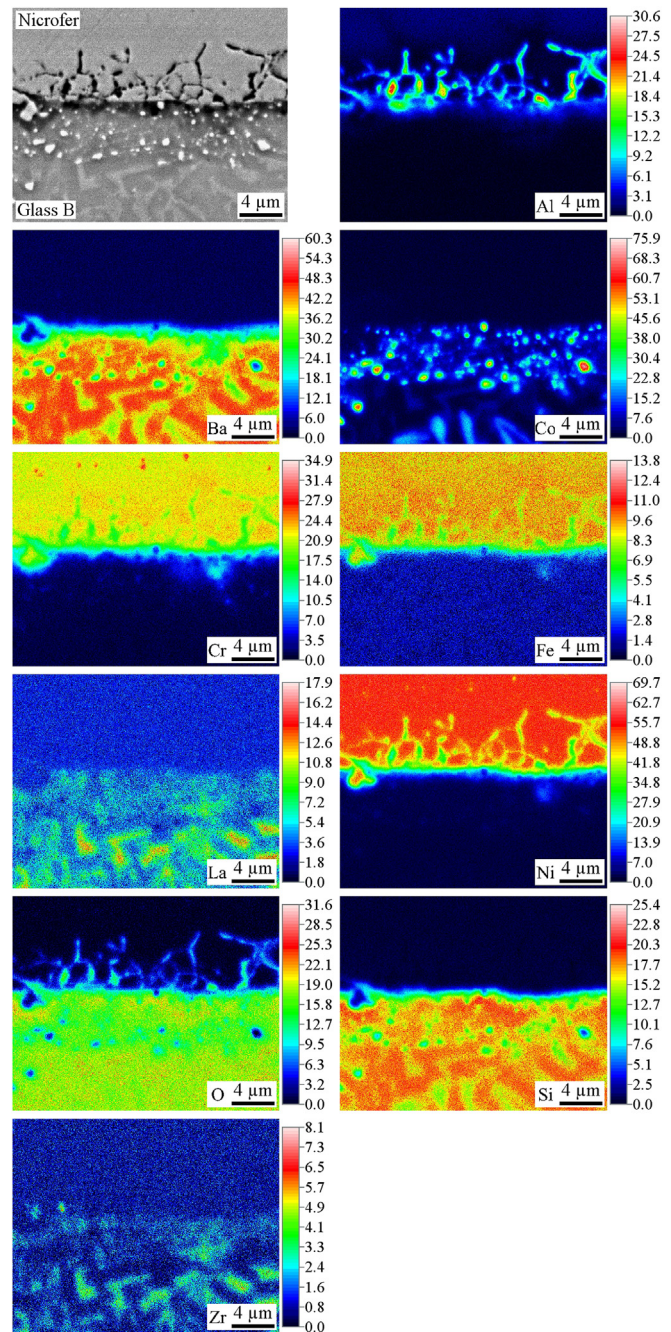


**Fig. 7.** SEM-micrograph and EDX mappings of sample B, sealed to the metal at 945 °C Al, Ba, Co, Cr, Fe, La, Ni, O, Si and Zr (the concentrations are given in wt%).

In comparison to Fig. 7, the interfacial layer does not occur in the same way. However, a strongly interconnected structure of dark appearance occurs in the metal near the boundary to the crystallized glass. This structure is strongly enriched in aluminum as well as in oxygen. In analogy to the boundary layer observed in Fig. 6, the interconnected structure seems to be alumina, however, due to the small size of this structure ( $<0.5 \mu\text{m}$ ), it cannot be excluded that also other elements occur in this phase. Furthermore, the chemical composition of the crystallized glass is not homogeneous within the whole volume. There are crystals which are strongly enriched in barium and silicon, while other parts of the microstructure are depleted in barium, but enriched in lanthanum, zirconia and cobalt. Near the interface to the metal, only minor concentrations of cobalt

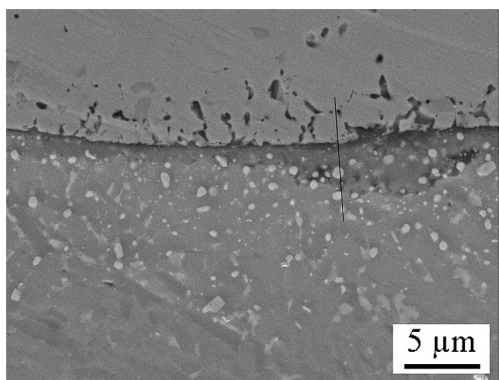


**Fig. 8.** SEM-micrograph of the interface of glass B, sealed to the metal at 945 °C and afterwards heat treated at 840 °C for 300 h. The black line marks the position of the line scan shown in Fig. 9.

are incorporated into the oxidic crystals, because most of the cobalt occurs as metallic particles. In both samples, i. e. those prepared from sample A and from sample B, nickel (from the Nicrofer<sup>®</sup> alloy) scarcely occurs in the oxidic phase.

The EDX-patterns in Figs. 6 and 7 show the interface between the glass-ceramic and the metal alloy. This interfacial layer causes strong adherence, which was measured, using the experimental setup, displayed in Fig. 1. On both metal plates, adherent glass is observed and the crack runs in between the crystallized glass and does not follow the interface metal/crystallized glass. That proves a strong adherence. The force necessary to fracture the sample was 780 N, which related to the area of the seal is attributed to a strength of 2.7 MPa.

After a heat treatment of 300 h at 840 °C in air all the sealed samples were undamaged. Figs. 8 and 9 show SEM-micrographs and an EDX-analysis of one of the samples. This sample was

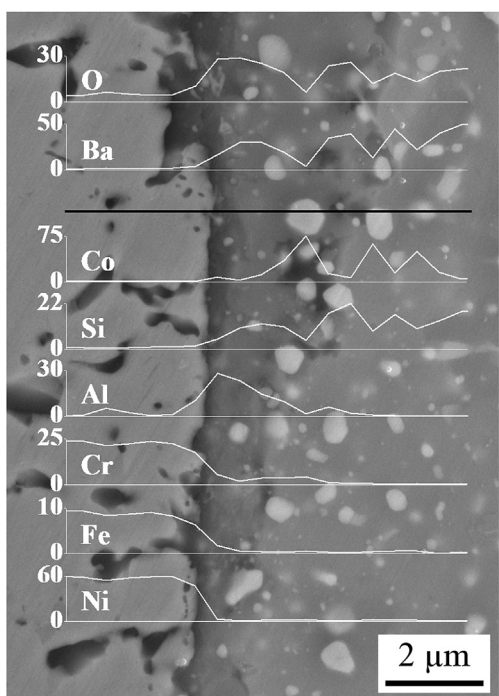


**Fig. 9.** EDX-line analyses of the interface of glass B and Nicrofer<sup>®</sup>. The samples were sealed at 945 °C for 40 min and afterwards heat treated at 840 °C for 300 h. The line scan was performed along the black line. The y-axes show the concentration in wt%.

prepared from glass B and the alloy. The sealing temperature was 945 °C. So this sample is comparable with the sample from Fig. 7. The uncertainties of the EDX-line scan are the same as described for the EDX-mappings. The interface shown in Figs. 8 and 9 does not show any significant difference compared to the interface shown in Fig. 7. There is a slight diffusion of chromiumoxide and alumina into the glass. The dimensions of the cobalt particles and the diffusion zones are marginally affected by the thermal treatment at 840 °C. Some cobalt particles occur in a larger distance from the interface in comparison with Fig. 7. This might be caused by the diffusion of small amounts of FeO into the glass, which is able to reduce the CoO to metallic cobalt.

Both studied glasses can easily be densified by thermal treatment. The crystallization process obviously does not disturb the densification by viscous flow. During subsequent crystallization, BaSi<sub>2</sub>O<sub>5</sub> as well as solid solutions Ba(Zn<sub>x</sub>Co<sub>2-x</sub>)Si<sub>2</sub>O<sub>7</sub> (in the case of sample A) or BaCo<sub>2</sub>Si<sub>2</sub>O<sub>7</sub> are formed. The thermal expansion coefficients are in the range suitable for sealing of nickel alloys such as Nicrofer<sup>®</sup>. The sealing process is very different from sealing processes reported up to now in the literature. Obviously a chemical reaction between the metal and the glass takes place. The aluminum of the metal (Nicrofer<sup>®</sup> contains approximately 2 wt% Al) is oxidized while the cobalt oxide present in the glassy phase is reduced to the metal. In principle, this process is known from the enameling of metals such as steel [28]. By contrast to enameling, however, the glass is crystallized during the sealing process which is a prerequisite for the high CTE necessary for the aimed applications. In the case of sample A which besides CoO also contains ZnO, an interfacial layer with some interconnected structures, is formed between the metal and the crystallized glass. In the case of sample B, at the same temperature, considerably more of such interconnected structures are formed in the metal. The interfacial layer as well as the interconnected structures are probably composed of alumina. Obviously, the adherence of the crystallized glass to the metal is strong as seen by the crack running through the crystallized glass during the fracture experiment.

#### 4. Conclusions

Glasses based on the systems BaO/CoO/SiO<sub>2</sub> and BaO/ZnO/CoO/SiO<sub>2</sub> were studied with respect to their sintering and crystallization behavior. They showed good densification and during crystallization phases such as BaSi<sub>2</sub>O<sub>5</sub> and Ba(Zn<sub>x</sub>Co<sub>2-x</sub>)Si<sub>2</sub>O<sub>7</sub> (in the case of sample A) or BaCo<sub>2</sub>Si<sub>2</sub>O<sub>7</sub> are formed. The crystallized samples exhibit CTEs (100–800 °C) of 14.0–14.6 × 10<sup>-6</sup> K<sup>-1</sup>. Sealing experiments showed strong adherence of the crystallized glass to the Nicrofer<sup>®</sup> alloy. In SEM-micrographs it is seen that aluminum from the alloy is oxidized and forms an alumina layer or other structures inside the Nicrofer<sup>®</sup> alloy, while cobalt from the glass is reduced to the metal. This leads to the formation of approximately spherical cobalt particles occurring near the Nicrofer<sup>®</sup> alloy. The number of cobalt particles increases with increasing sealing temperature. During fracture of sealed Nicrofer<sup>®</sup> plates, the crack runs through the glass and not through the interface metal/crystallized glass. The thermal expansion coefficient of the crystallized seal can be adjusted by the cobalt concentration.

#### References

- [1] M. Kerstan, M. Müller, C. Rüsel, *Mater. Res. Bull.* 46 (2011) 2456–2463.
- [2] M.K. Mahapatra, K. Lu, *Mater. Sci. Eng. R* 67 (2010) 65–85.
- [3] A. Hunger, G. Carl, A. Gebhardt, C. Rüsel, *J. Non Cryst. Solids* 354 (2008) 5402–5407.
- [4] A. Hunger, G. Carl, A. Gebhardt, C. Rüsel, *Mater. Chem. Phys.* 122 (2010) 502–506.

- [5] Y.S. Chou, J.W. Stevenson, P. Singh, J. Electrochem. Soc. 154 (2007) B644–B651.
- [6] S. Ghosh, A.D. Sharma, P. Kundu, R.N. Basu, J. Electrochem. Soc. 155 (2008) B473–B478.
- [7] K.D. Meinhardt, D.S. Kim, Y.S. Chou, K.S. Weil, J. Power Sources 182 (2008) 188–196.
- [8] M.J. Pascual, A. Guillet, A. Durán, J. Power Sources 169 (2007) 40–46.
- [9] S.B. Sohn, S.Y. Choi, G.H. Kim, H.S. Song, G.D. Kim, J. Am. Ceram. Soc. 87 (2004) 254–260.
- [10] Z. Yang, K.S. Weil, D.M. Paxton, J.W. Stevenson, J. Electrochem. Soc. 150 (2003) A1188–A1201.
- [11] J.W. Fergus, Mater. Sci. Eng. A 397 (2005) 271–283.
- [12] E. Ivers-Tiffée, A. Weber, D. Herbstritt, J. Eur. Ceram. Soc. 21 (2001) 1805–1811.
- [13] S.F. Wang, C.M. Lu, Y.C. Wu, Y.C. Yang, T.W. Chiu, Int. J. Hydrogen Energy 36 (2011) 3666–3672.
- [14] S. Sakuragi, Y. Funahashi, T. Suzuki, Y. Fujishiro, M. Awano, J. Power Sources 185 (2008) 1311–1314.
- [15] C. Lara, M.J. Pascual, M.O. Prado, A. Durán, Solid State Ionics 170 (2004) 201–208.
- [16] M. Kerstan, C. Rüssel, J. Power Sources 196 (2011) 7578–7584.
- [17] S.T. Reis, M.J. Pascual, R.K. Brow, C.S. Ray, T. Zhang, J. Non Cryst. Solids 356 (2010) 3009–3012.
- [18] M.K. Mahapatra, K. Lu, J. Power Sources 195 (2010) 7129–7139.
- [19] M. Kerstan, M. Müller, C. Rüssel, J. Solid State Chem. 188 (2012) 84–91.
- [20] C. Sun, R. Hui, J. Roller, J. Solid State Electrochem. 14 (2010) 1125–1144.
- [21] F. Tietz, Ionics 5 (1999) 129–139.
- [22] D. Skarmoutsos, A. Tsoga, A. Naoumidis, P. Nikolopoulos, Solid State Ionics 135 (2000) 439–444.
- [23] J. Wu, X. Liu, J. Mater. Sci. Technol. 26 (2010) 293–305.
- [24] B.W. King, H.P. Tripp, W.H. Duckworth, J. Am. Ceram. Soc. 42 (1959) 504–525.
- [25] R.S. Roth, E.M. Levin, J. Research Natl. Bur. Stand. 62 (1959) 193–200.
- [26] M. Kerstan, C. Thieme, M. Grosch, M. Müller, C. Rüssel, J. Solid State Chem. 207 (2013) 55–60.
- [27] Z.H. Jia, A.K. Schaper, W. Massa, W. Treutmann, H. Rager, Acta Crystallogr. B Struct. Sci. 62 (2006) 547–555.
- [28] D.G. Moore, J.W. Pitts, J.C. Richmond, W.N. Harrison, J. Am. Ceram. Soc. 37 (1954) 1–6.